

UDC 621.739.6:669.245

## EFFECT OF TCP-PHASES ON THE TENSILE FRACTURE BEHAVIOR OF SINGLE-CRYSTAL NICKEL ALLOY ZhS36-VI [001]

V. P. Kuznetsov,<sup>1,2</sup> V. P. Lesnikov,<sup>1,2</sup> I. P. Konakova,<sup>1</sup> and N. A. Popov<sup>1</sup>

Translated from *Metallovedenie i Termicheskaya Obrabotka Metallov*, No. 9, pp. 40 – 43, September, 2014.

Results of a study of the special features of tensile fracture of single-crystal nickel alloy ZhS36-VI [001] after high-temperature holds are presented. The role of the tcp-phases in fracture of the single-crystal nickel alloy is considered.

**Key words:** single-crystal refractory nickel alloy, structure, phase composition, tcp-phases, fractography.

### INTRODUCTION

The main problem of castable single-crystal refractory nickel alloys (RNA) with additives of Ta and Re is the thermal stability of their structure and phase composition in operation. Under the action of high temperatures (above 1050°C) and stresses the particles of the  $\gamma'$ -phase coalesce and intergrow yielding a raft structure, and dissolve. In operation, complexly alloyed refractory alloys may acquire tcp-phases of different types, namely, a rhombohedral  $\mu$ -phase, a tetragonal  $\sigma$ -phase and an orthorhombic  $P$ -phase [1 – 6].

We have studied the formation of tcp-phases of different morphology in single-crystal alloy ZhS36-VI after a hold in the range of 1050 – 1200°C in [7]. It has been shown that these are  $\mu$ -phases of type  $(\text{Ni}, \text{Co})_7(\text{Cr}, \text{W}, \text{Re}, \text{Mo})_6$  with an average composition (in wt.%) of 23Ni – 8Co – 40W – 20Re – 4Mo – 5Cr. The  $\mu$ -phases form intensely in the arms of dendrite cells and grow in the  $\mu$ -phase matrix enriched with Al, Ti, and Ta. The chemical composition and the morphology of the  $\mu$ -phases are determined by the chemical composition of the RNA and by the temperature-and-time range. Systematized data on the effect of tcp-phases on the tensile fracture behavior of the alloy are lacking.

The aim of the present work was to study the effect of the tcp-phases formed in alloy ZhS36-VI [001] and the special features of its fracture in short-term mechanical tests at 20 and 975°C.

### METHODS OF STUDY

Castable refractory nickel alloy ZhS36-VI with a rhenium additive is used to cast cooled turbine blades with crystallographic orientation CGO [001], which operate at 1100 – 1150°C. The average chemical composition of ZhS36-VI [7] is 4.0% Cr, 9.0% Co, 1.2% Mo, 11.7% W, 2.0% Re, 1.1 Nb, 1.1% Ti, 5.8% Al, the remainder Ni.

Single-crystal test pieces with CGO [001] were obtained under industrial conditions in a UVNK-8P unit without liquid-metal coolant at a rate of crystallization equal to 3 mm/min. The crystallographic orientation was specified by seed crystals of a Ni-W alloy. The deviation of the growing structure from crystallographic orientation [001] did not exceed 4°. The heat treatment of alloy ZhS36-VI is described in [7].

Cast billets with  $\varnothing$  14 mm after the heat treatment were subjected to high-temperature holds at 1050 – 1300°C in the furnace air atmosphere. They were used to fabricate standard cylindrical test pieces with functional part 5 mm in diameter for determining the mechanical properties.

The characteristics of the mechanical properties in short-term tensile tests at 20 and 975°C were determined in accordance with the GOST 1497–84 and GOST 9651–81 Standards using an Instron 3382 testing machine.

The metallographic study and the analysis of the chemical composition of the phases were performed by the methods of scanning electron microscopy (SEM) using a “Jeol JSM 6490 LV” device with an “Oxford Inca Drycool” attachment for microscopic x-ray spectrum analysis (MXRSA).

The electron microscope studies of the fine structure of the alloy were performed by the method of transmission

<sup>1</sup> Ural Federal University after the First President of Russia B. N. Eltsyn, Ekaterinburg, Russia.

<sup>2</sup> “TURBOMET” Company, Ekaterinburg, Russia (e-mail: turbomet@e1.ru).

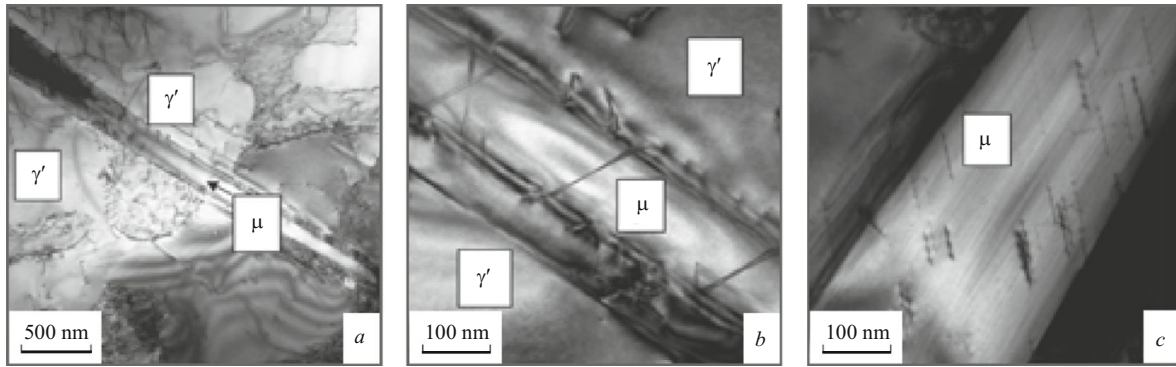


**Fig. 1.** Light-background image of the fine structure of  $\mu$ -phases in alloy ZhS36-VI after a hold of 500 h at 1150°C.

electron microscopy (TEM) of thin foils with the help of “EMV-100L” and “Jeol JEV-2100” devices.

## RESULTS AND DISCUSSION

After a complete heat treatment (CHT) alloy ZhS36-VI has a typical homogeneous disperse ( $\gamma + \gamma'$ ) structure with a high volume fraction of particles of a hardening  $\gamma'$ -phase (70 – 75 vol.%) 0.3 – 0.4  $\mu\text{m}$  in size. The particles of the  $\gamma'$ -phase have a characteristic cuboid shape. Electron diffraction and microdiffraction analysis shows that the particles of the  $\gamma'$ -phase are arranged in single-crystal directions of type  $[100]_{\gamma'}$ . The alloy does not have observable tcp phases [5].

The main feature of the structure of alloy ZhS36-VI  $[001]$  after a long high-temperature hold is formation of  $\mu$ -phases in the temperature range of 1050 – 1200°C (see Fig. 1).

We can observe extinction contours at the point of a needle of the  $\mu$ -phase (Fig. 1a), which are connected with the elastic stresses in the  $\gamma'$ -phase arising upon growth of the  $\mu$ -phase. The  $\mu$ -phase contains flat crystal lattice flaws

(twins or stacking faults in Fig. 1b and dislocations in Fig. 1c). In the adjoining volumes of the matrix we can observe single dislocations as well as parallel dislocations over the  $\mu/\gamma'$  interface. The crystal lattices of the  $\mu$ - and  $\gamma'$ -phases obey a strict crystallographic orientation relation [7]. The morphological and crystallographic characteristics of the  $\mu$ -phases reflect their growth in the  $\gamma'$ -phase; regions of contact between the  $\mu$ -phase and the  $\gamma$ -phase have not been detected.

The results of the determination of the composition of the phases in alloy ZhS36-VI (see Table 1) show that the primary  $\gamma'$ -phase is enriched with Al during the thermal holds at simultaneous decrease in the content of W and Re in it. On the contrary, the matrix of the  $\gamma'$ -phase surrounding the  $\mu$ -phase is enriched with W and Re as compared to the primary  $\gamma'$ -phase, and the content of Al in it decreases.

The ( $\gamma + \gamma'$ ) structural component between the precipitates of the  $\mu$ -phases has a chemical composition close to that of the alloy in the arms of dendritic cells. This proves that the  $\mu$ -phases are located primarily in dendrite arms.

**TABLE 1.** Composition of Structural Components of Alloy ZhS36-VI  $[001]$

Heat treatment	Structural component (phase)	Content of elements (wt.%) according to the data of microscopic x-ray spectrum analysis								
		Al	Ti	Cr	Co	Ni	Nb	Mo	W	Re
CHT	Average chemical composition	5.80	1.10	4.00	9.00	64.10	1.10	1.20	11.70	2.00
	Structural component ( $\gamma + \gamma'$ ) in arms	4.95	1.25	4.04	8.55	59.46	0	1.41	15.36	4.49
	Structural component ( $\gamma + \gamma'$ ) in arm spacing	6.18	1.22	3.64	7.98	63.86	1.20	1.27	11.74	2.71
CHT + 500-h hold at 1150°C	Coarse primary $\gamma'$ -phase	7.41	1.57	2.61	7.60	67.65	1.62	1.19	10.35	0
	$M$ -phase	0.62	0.36	4.22	7.69	21.33	0	3.68	43.53	18.66
	$\gamma'$ -phase around the $\mu$ -phase	0.62	1.72	1.93	6.79	67.36	1.58	1.09	11.43	1.11
	( $\gamma + \gamma'$ ) between $\mu$ -phases	3.81	0.62	5.26	10.07	58.61	0.62	2.01	15.62	3.14
	Layers of ( $\gamma_n + \gamma'_n$ ) secondary mixture	4.49	1.17	4.37	9.29	61.31	1.33	2.27	14.08	1.74

It has been shown in [8] that the resistance of alloy ZhS36-VI to deformation after a high-temperature hold increases upon a change in the composition of the  $\gamma'$ -phase and growth in the energy and in the density of the  $\gamma/\gamma'$  interfaces (the size factor) due to formation of a ( $\gamma_n + \gamma'_n$ ) nanosize mixture and elevation of the internal stresses. The alloy undergoes nanosize hardening. Tension at  $t = 20^\circ\text{C}$  raises the rupture strength ( $\sigma_r$ ) of the alloy considerably (by a factor of about 1.5), and the ductility  $\delta$  remains at a high level. Similar changes in the mechanical properties ( $\sigma_{0.2}$ ,  $\sigma_r$  and  $\delta$ ) are observed after testing at  $975^\circ\text{C}$ .

We established that the test pieces of carbonless alloy ZhS36-VI

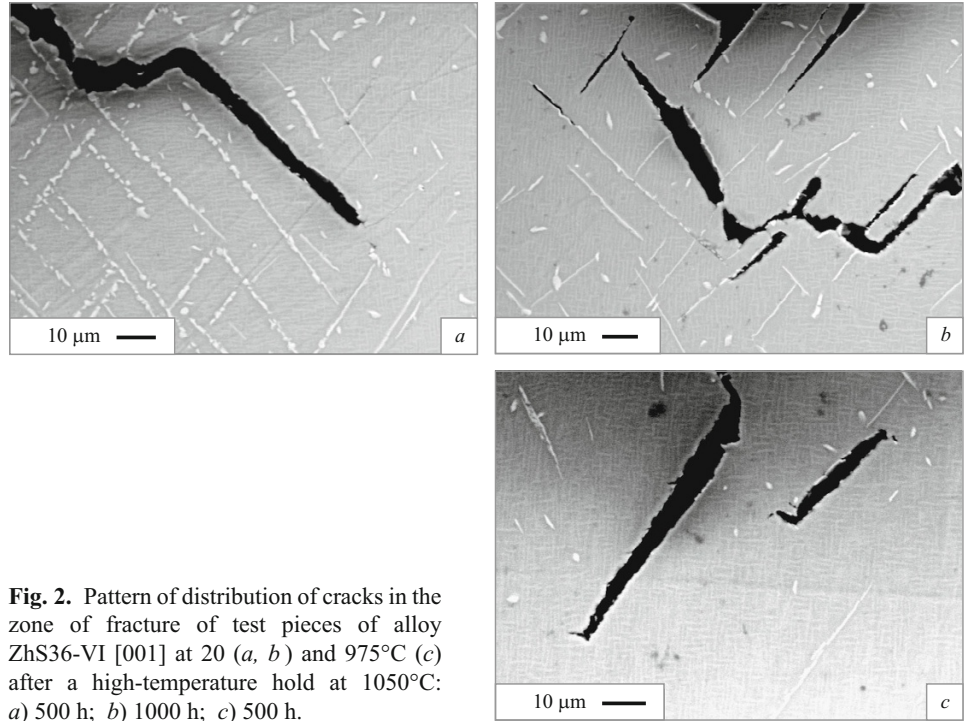


**Fig. 2.** Pattern of distribution of cracks in the zone of fracture of test pieces of alloy ZhS36-VI [001] at 20 (*a*, *b*) and  $975^\circ\text{C}$  (*c*) after a high-temperature hold at  $1050^\circ\text{C}$ : *a*) 500 h; *b*) 1000 h; *c*) 500 h.

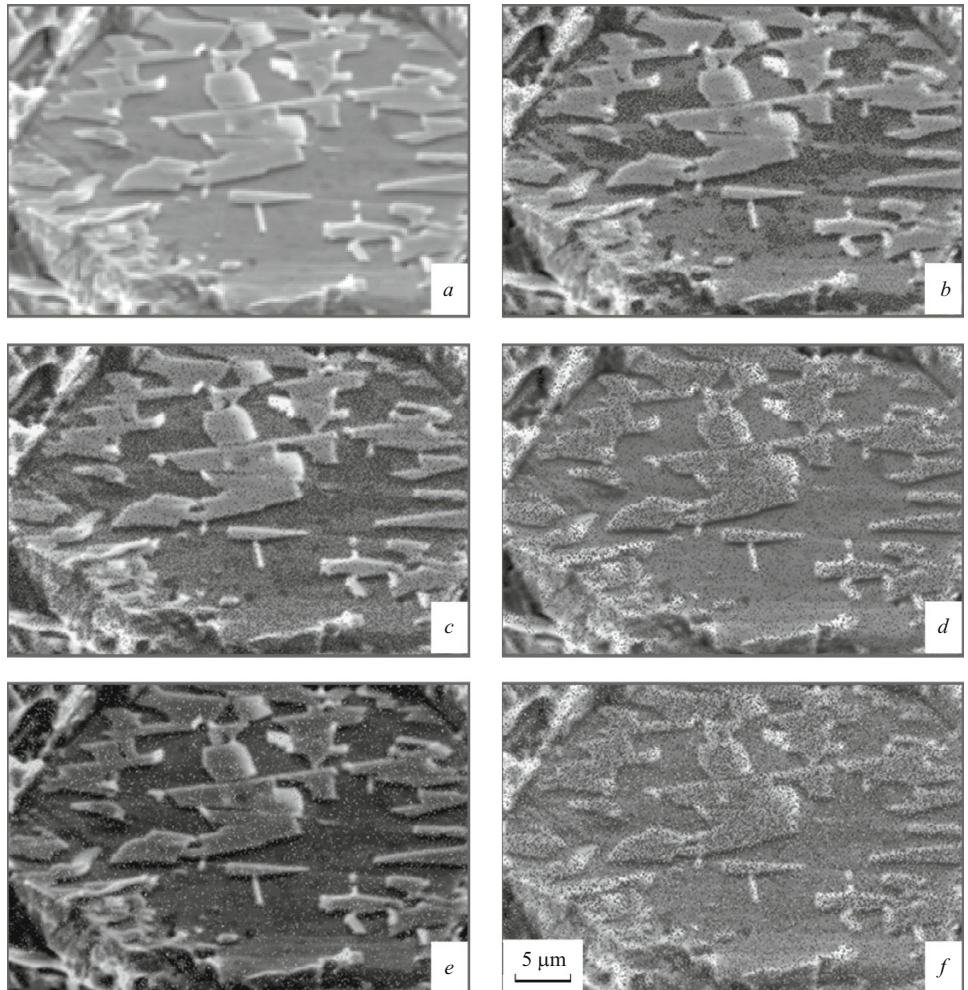
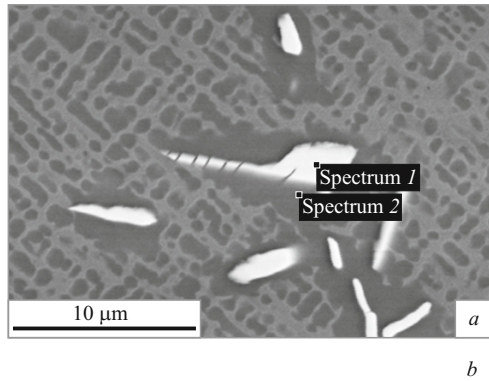


**Fig. 3.** Structure (*a*) and distribution of chemical elements in the mode of mapping of structural components in a fracture of alloy ZhS36-VI [001] (*b*–*f*) after tension at  $20^\circ\text{C}$  with a preliminary 100-h hold at  $1150^\circ\text{C}$ : *b*) Al; *c*) Ni; *d*) Re; *e*) W; *f*) W + Re.





Composition of  $\mu$ - and  $\gamma'$ -phases in alloy ZhS36-VI, wt. %

Analyzed zone	Al	Ti	Cr	Co	Ni	Nb	Mo	W	Re
Spectrum 1 – $\mu$ -phase with microcracks	0.26	0.00	4.58	7.65	17.03	0.00	2.81	49.35	18.31
Spectrum 2 – coarse film $\gamma'$ -phase	6.75	1.70	1.92	6.96	65.66	1.59	1.14	12.35	1.94

**Fig. 4.** Fine structure (a) of alloy ZhS36-VI [001] and chemical composition of the phases (b) in the zone of fracture at 20°C after a 200-h hold at 1150°C.

with CGO [001] fractured after high-temperature holds in tensile tests at 20 and 975°C due to formation and propagation of cracks over the interface of a “coarse”  $\gamma'$ -phase and a  $\mu$ -phase (Fig. 2).

Mapping of the fracture surfaces showed that  $\mu$ -phases enriched with the refractory elements of the alloy (Cr, W, Re and Mo) and depleted of Ni, Al and Ti were located on the surface of the “coarse”  $\gamma'$ -phase (see Fig. 3). Film precipitates of the “coarse”  $\gamma'$ -phase enveloped the  $\mu$ -phases formed in the high-temperature hold. The depletion of the  $\gamma$ -phase of Re, W and Mo lowered the efficiency of the solid-solution hardening; the resistance to the slip of dislocations decreased and this lowered the strength of the alloy.

Under the action of tensile stresses at 975°C diffusion pores form in the  $\gamma'$ -phase in the region of fracture of test pieces of alloy ZhS36-VI [001]. The diffusion pores arising in the coarse  $\gamma'$ -phase have octahedral faceting over close-packing planes  $\{111\}$  of the  $\text{Ni}_3\text{Al}$  intermetallic [9] and are additional sources of nucleation of microcracks in RNA.

When the test pieces are stretched after a high-temperature hold, the fracture zone exhibits cracking of the formed  $\mu$ -phases (Fig. 4).

The electron diffraction patterns obtained in the study of the CGO of alloy ZhS36-VI [001] always contain reflections of zone [001] and close regions in the working zones of the test pieces after tension, which indicates absence of substantial deviations from the initial orientation of the longitudinal axis of the pieces studied from direction [001].

## CONCLUSIONS

1. The  $\mu$ -phases formed under high-temperature holds in alloy ZhS36-VI [001] grow in the  $\gamma'$ -phase. No region of contact between the  $\mu$ -phases and the  $\gamma$ -phase has been detected.

2. During a thermal hold the primary  $\gamma'$ -phase is enriched with Al at simultaneous decrease in the content of W and Re in it. The  $\gamma'$ -phase matrix enveloping the  $\mu$ -phase is enriched with W and Re as compared to the primary  $\gamma'$ -phase, and the content of Al in it is reduced. The ( $\gamma + \gamma'$ ) structural component between the  $\mu$ -phases has a chemical composition close to the composition of the alloy in dendrite cell arms.

3. Fracture of test pieces of alloy ZhS36-VI [001] after a high-temperature hold and tensile tests at 20 and 975°C occurs due to nucleation and propagation of cracks over the “coarse”  $\gamma'$ -phase/ $\mu$ -phase interface.

4. A study of fracture surfaces in a mapping mode has shown that  $\mu$ -phases enriched with refractory Cr, W, Fe and Mo and depleted of Ni, Al and Ti are located on the surface of the “coarse”  $\gamma'$ -phase. Film precipitates of the “coarse”  $\gamma'$ -phase envelop the  $\mu$ -phases formed in the alloy under high-temperature holds. The efficiency of the solid-solution hardening decreases due to the depletion of the  $\gamma$ -phase of Re, W and Mo; the resistance to the dislocation slip becomes lower and the strength of the alloy is reduced.

## REFERENCES

1. C. T. Sims and W. Hagel, *Refractory Alloys* [in Russian translation], Metallurgiya, Moscow (1976), 567 p.
2. C. T. Sims, N. S. Stoloff, and W. C. Hagel, *Superalloys II. Refractory Materials for Aerospace and Industrial Power Plants, Book 1*, [in Russian], Metallurgiya, Moscow (1995), 384 p.
3. R. E. Shalin, I. L. Svetlov, E. B. Kachanov, et al., *Single Crystals of Nickel Refractory Alloys* [in Russian], Mashinostroenie, Moscow (1997), 336 p.
4. E. N. Kablov, *Cast Blades of Gas Turbine Engines: Alloys, Technologies, Coatings* [in Russian], MISiS, Moscow (2001), 632 p.
5. V. P. Kuznetsov, V. P. Lesnikov, V. E. Zamkovoy, and A. S. Koraykovtsev, *Structure and Strength Properties of Nickel-Base Single Crystal Alloys with Tantalum and Rhenium* [in Russian], “Kvist,” Ekaterinburg (2010), 140 p.
6. E. N. Kablov, N. V. Petrushin, M. B. Bronfin, and A. A. Alekseev, “Special features of single-crystal refractory nickel alloys with rhenium,” *Metally*, No. 5, 47 – 57 (2006).
7. V. P. Kuznetsov, V. P. Lesnikov, M. S. Khadyev, et al., “Structure and phase transformations in single-crystal alloy ZhS36-VI [001] after a hold in the temperature range of 1050 – 1300°C,” *Metalloved. Term. Obrab. Met.*, No. 2, 38 – 44 (2012).
8. V. P. Kuznetsov, V. P. Lesnikov, I. P. Konakova, et al., “Volume nanophase hardening in single-crystal nickel alloy ZhS36-VI [001] after high-temperature holds,” *Metalloved. Term. Obrab. Met.*, No. 4, 3 – 6 (2014).
9. M. R. Orlov, “Physicochemical features of formation of heat-induced pores and operating capacity of single-crystal turbine blades,” *Deform. Razrush. Mater.*, No. 6, 43 – 48 (2008).